MATERIAL PROPERTIES INFLUENCING THE REACTIVITY OF ACTIVATED CARBONS: THERMAL ANALYSIS, HRTEM STUDY AND STATISTICAL MODELLING

Thangavelu Jayabalan, Pascaline Pré, Valérie Héquet, GEPEA UMR-CNRS 6144, Ecole des Mines de Nantes, BP-20722 4 Rue Alfred Kastler, Nantes-44307, France.
Jean Noël Rouzaud, Ecole Normale Supérieure de Paris, Laboratoire de Géologie, UMR 8538 CNRS-ENS , 24 Rue Lhomond, 75231 Paris, France.
Pierre Le Cloirec, Université Européenne de Bretagne - Ecole de Chimie de Rennes (ENSCR), UMR CNRS 6226 "Sciences Chimiques de Rennes", Campus de Beaulieu, Avenue du général Leclerc, 35700 Rennes, France.

Abstract

The aim of this work is to understand the influence of textural, chemical and structural properties influencing the reactivity of activated carbons. Multiscale organization of activated carbons were studied using a high resolution transmission electron microscopy (HRTEM) and their quantitative structural data like individual fringe length, interlayer spacing and number of stacked layers in a coherent domain were extracted using an in house image analysis procedure. Intrinsic properties like the S_{BET}, pore volume, micropore width and chemical composition were also measured. The reactivity of the carbon samples in air were quantified using thermogravimetry coupled with a differential scanning calorimetry, oxidation and ignition temperatures were measured. The organization of the graphitic structure and the properties of the activated carbon samples were dependant on the mode of activation and the nature of the material. The results suggest that oxygen to carbon ratio in the form of surface oxygenated groups and the characteristics of the basic structural units influenced the reactivity of activated carbons. The structure of highly stable carbons was found to contain less oxygen to carbon ratio with larger and better stacked polyaromatic layers.

1. Introduction

Activated carbons are widely used in heterogeneous catalysis, personal protection equipment, vehicle filters and for the removal of VOC's and odours from industrial effluents. The main drawback with these materials is the early oxidation and ignition due to external heating, exothermal adsorption and chemical reactions. Ignition risks are commonly found for activated carbons packed in filters, mainly caused by certain types of contaminants that are filtered or adsorbed. Extensive literature sources are available for incidents of fires and thermal runaways encountered with activated carbon beds in service, idle condition and also during the handling and regeneration of the spent carbon (Naujokas, 1985; Delage *et al*., 2000; Zerbonia *et al*., 2001). Fires were also reported during transit on board ship for chemically activated carbons (Bowes and Cameron, 1971).

Based on these contexts, a laboratory study is undertaken to evaluate how the textural, chemical and structural properties contribute to the reactivity of the activated carbons. In the recent years, many studies were accomplished in an effort to link the structural properties of carbon materials with their reactivity due to the advancement of the characterization techniques. Different experimental techniques like the HRTEM (high resolution transmission electron microscopy), coupled with adsorption experiments with molecules of various sizes and shapes have confirmed that the structure of nanocarbons such as the activated carbons consists of short, distorted and weakly stacked aromatic sheets with spaces between the layers corresponding to the micropores between them. The structural organisation of the activated carbons also plays an important role in the reactivity of the material and therefore it is important to take into account the effect of structural properties.

Several test methods can be found in the literature for characterising the oxidation reactivity of the activated carbons. These methods enable to determine various reactivity parameters representative of the tendency of the carbonaceous materials to oxidation and self ignition. The characterization of oxidation and ignition process of activated carbons at elevated temperatures was extensively studied by Suzin *et al*., 1999. Two regions of interest were defined which describe the oxidation process at relatively low temperature (PIO) followed by ignition at higher temperature (SIT). The PIO is described as Point of Initial Oxidation where the carbon starts to oxidize significantly and the SIT is described as the Spontaneous Ignition Temperature where the combustion of carbon takes place in a self sustaining manner. This test method is mainly used for the comparison of the ignition characteristics of the different activated carbons and should not be taken as the true oxidation and ignition temperatures as they are dependant on the operating conditions of activated carbons.

The objective of the present work therefore is to study the relationships between the chemical, textural and structural properties of activated carbons and their reactivity. The general trends of the various properties of activated carbons are plotted against the reactivity parameters like SIT and PIO. This is followed by establishing quantitative statistical correlations with the material properties and their oxidation and ignition reactivities. This approach is contributing to the understanding of the important intrinsic properties influencing the reactivity leading to oxidation and spontaneous ignition of activated carbons.

2. Experimental

2.1. Materials

Seventeen different activated carbons were selected for this study based on the nature of the raw material and the mode of activation applied. All of them were produced from the carbonization at 800 °C-1000 °C in the absence of oxygen of various synthetic and natural raw materials (coconut, peat, coke, wood, olive stone and polyacrylonitrile fibre) followed by physical or chemical activation. Physical activation was carried out using steam or CO_2 gases and the chemical activation was performed using concentrated solutions like H_3PO_4, $ZnCl_2$, and H_2SO_4. The polymer based activated carbons were prepared by blending PAN (polyacrylonitrile fibre) and coal tar pitch CTP and carbonizing at 520 °C for 2 hours and the resultant chars were activated using steam at 800 °C.

Table 1. General characteristics of activated carbon samples.

Sample Name	Manufacturer	Raw material	Mode of activation
NC-50	PICA	Coconut shell	Physical
NC-60	PICA	Coconut shell	Physical
NC-100	PICA	Coconut shell	Physical
RB-2	NORIT	Peat	Physical
BPL	CHEMVIRON	Coal	Physical
GF-40	NORIT	Olive stone	Chemical
BC-120	PICA	Wood	Chemical
PICABIOL	PICA	Wood	Chemical
CTP-A	LCSM Nancy	Coal tar pitch	Physical
CTP-PAN-3 :1-A	LCSM Nancy	Coal tar pitch and polyacrylonitrile fibre	Physical
CTP-PAN-1 :1-A	LCSM Nancy	Coal tar pitch and poyacrylonitrile fibre	Physical
PAN-A	LCSM Nancy	poyacrylonitrile fibre	Physical
PAN-C	LCSM Nancy	poyacrylonitrile fibre	Physical
Carbonized coconut shell	PICA	Coconut shell	Non-activated

2.2 Structural characterization

The nanostructural characterization of the activated carbons was carried out using a Jeol 2011 HRTEM (acceleration voltage 200 kV, resolution in the lattice fringe mode 0.14 nm). The HRTEM allows to study the multiscale organisation of the carbon materials and to quantify them thanks to a lab made image analysis. The samples were first grounded in a small agata mortar, dispersed in ethanol and a drop of solution was then deposited on a classical TEM copper grid, previously covered by a holey amorphous carbon film. A software of HRTEM analysis specially developed , was used to obtain quantitative structural information (Rouzaud and Clinard, 2002). The raw HRTEM images were recorded on classical negatives and a part of this image is sampled and digitalised (256 grey levels, resolution 4000 pixels per inch). With the help of an improved version of the visolog (Noesis) commercial software, an homogenous image without background noise is first obtained, and then binarised and skeletonized; each fringe is now one pixel-large (the size of one pixel for this work : 0.017 nm). The skeletonized pixel based image is then transformed into a vectorial image and each fringe is analysed individually in relation to its neighbours, thanks to a lab-made software. Careful analysis is done taking into account different criterions to avoid artefacts (for instance fringes smaller than 0.25 nm, i.e. the size of a single aromatic ring, were considered without physical sense and eliminated). Pairs of fringes were here considered as stacked layers to form coherent domains (i.e. Basic Structural Units or BSU), only if their angle is smaller than 15 ° and their interlayer spacing narrower than 0.6 nm. The software allows to obtain de-averaged data on fringe length, interlayer spacing and number of stacked layers in a coherent domain with great advantage than the usual X-ray diffraction techniques which give poor information on averaged data.

Figure 1. HRTEM image analysis: structural analysis showing coherent domain limits: L is the individual fringe length, L_a is the width of the coherent domain, L_c is its height related to *d* which is the interlayer spacing and N is the number of stacked layers within a domain.

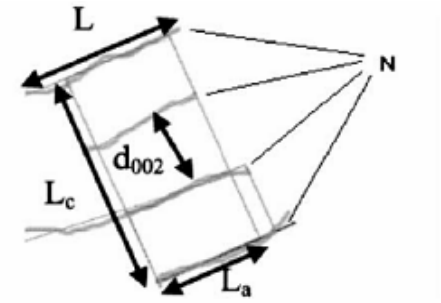

Figure 2. HRTEM images of some of the carbon samples used for the study (image size 16 nm X 16 nm)

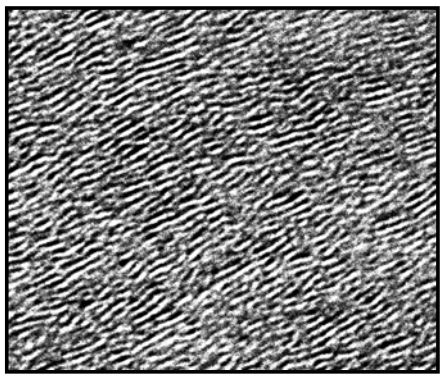

(a) CTP-A

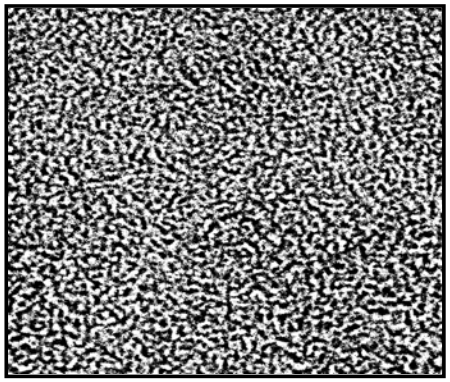

(b) Carbonized coconut shell

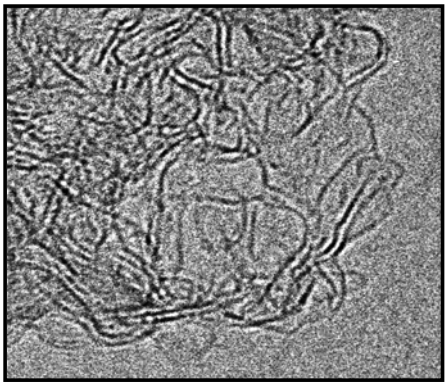

(c) NC-100

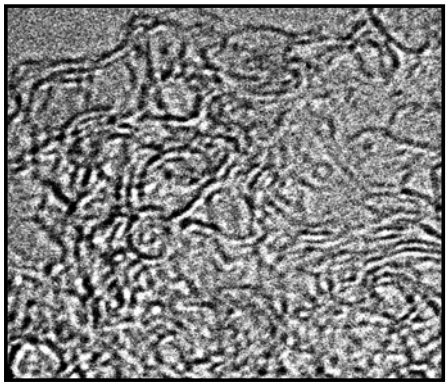

(d) RB-2

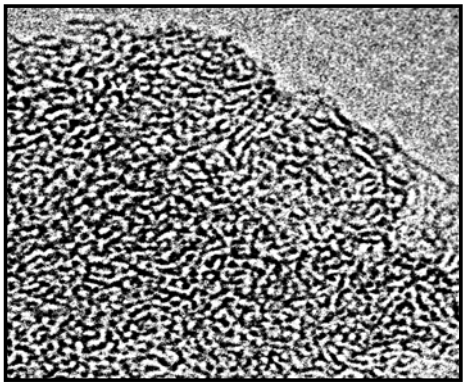

(e) BC-120

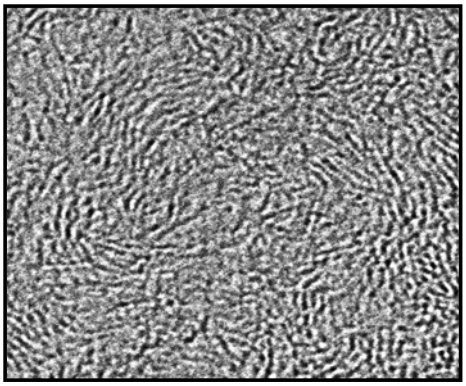

(f) PAN-A

Table 2. Average structural parameters of carbon samples obtained from the in house image analysis procedure.

Sample	% Non Stacked Layers (NSL)	L > 2.85 (Å)	L > 4.9 (Å)	L > 10 (Å)	La (Å)	Lc (Å)	N	dmoy (Å)
RB-2	57	5.8	8.4	14.5	4.6	6	2.5	4.2
PAN-A	59	6.4	9	14.7	3.9	5.3	2.4	3.9
PAN-C	47	6.3	8.8	14.4	4.3	6.9	2.8	3.8
CTP-A	14	9.7	12.3	18.1	7.2	10.3	3.7	3.8
CTP-1 :1-A	60	5.8	8.4	13.8	3.8	5.6	2.5	3.9
NC-60	53	6.3	8.9	14.4	4.4	5.9	2.5	4.0
NC-100	51	6.1	9.1	16.5	4.7	5.4	3.9	3.9
NC-50	50	5.6	8.4	14.5	4.2	6	2.6	3.8
BPL	58	6	8.6	15	3.7	5.4	2.5	3.8
BC-120	65	5.5	7.7	13.3	3.5	4.9	2.2	3.9
GF-40	74	5.4	7.7	12.6	3	4.7	2.2	4
Picabiol	66	4.8	7.1	15.2	3.4	4.5	2.1	4.1

2.3. Chemical and textural characterization

2.3.1. Chemical composition

The mass ratios over carbon for the elements such as oxygen, hydrogen, nitrogen and sulphur of the carbon samples were measured using Thermofinnigan Flash EA-112 elementary analyser.

2.3.2. Porosity characteristics

The volume of larger pores (including macro and mesopores) of the AC samples was measured by mercury porosimetry (Micrometrics Auto pore IV 9500). The experimental error was found to be less than 10%. The microporous nanostructure of the AC samples was determined from nitrogen adsorption isotherms at 77 K (Micrometrics ASAP 2010 adsorption instrument). Prior to the analysis, the carbon samples were degassed at 250 °C for about 48 hours. The specific surface area was measured using the BET model from the adsorption of gases on the surface of the material. The volume of the micropores was measured from the t-plot or De Boer method that provides a simple mean of comparing the shape of a given adsorption isotherm with that of a standard non-porous solid (Lecloux, 1975; Olivier, 1995). The average width of the micropore was evaluated from the Density Functional Theory (DFT) (Lastoskie, 1993). Repeatability tests showed that the specific surface area, as well as the volume and the width of the micropores were determined with an accuracy of about 10%.

The results of the porosity characteristics and chemical composition can be found in table 3.

Table 3. Chemical and porosity characteristics of carbon samples tested.

Sample	O/C (%)	H/C (%)	N/C (%)	Volume of micropores (cm^3/g)	Average width of micropores (nm)	Surface area (m^2/g)	Porous volume (cm^3/g)
NC-50	1.72	0.52	0	0.36	1.35	1078	1.28
NC-60	3.60	0.30	0.04	0.32	0.97	1220	0.35
NC-100	3.30	0.53	0	0.27	1.11	1803	0.47
RB-2	5.90	0.32	0.20	0.35	0.92	1012	0.34
BPL	4.10	0.20	0.30	0.30	0.93	1106	0.40
GF-40	34.60	2.64	0.30	0.29	1.15	1718	0.80
BC-120	35.40	2.72	0.01	0.33	1.12	1975	1.50
PICABIOL	40.60	2.70	0	0.24	1.38	1534	1.34
CTP-A	1.72	3.08	0.70	0.04	1.30	102	0.07
CTP-PAN-3 :1-A	3.10	0.86	5.70	0.20	1.32	468	0.25
CTP-PAN-1 :1-A	7.20	1.22	9.20	0.21	1.11	482	0.27
PAN-A	13.40	1.12	15.5	0.26	1.15	515	0.27

PAN-C	6.30	1.63	21.70	<<	<<	<<	<<
CTP-PAN-3 :1-C	2.40	1.21	7.10	<<	<<	<<	<<
CTP-C	0.70	1.27	0.75	<<	<<	<<	<<
CTP-PAN-1 :1-C	3.30	1.20	13.40	<<	<<	<<	<<
Carbonized coconut shell	12.40	1.07	0.07	<<	<<	<<	<<

2.4. Thermal analysis

The instrument ATG-DSC, SETARAM-111 was used for the determination of the Point of Initial Oxidation (PIO) and the Self Ignition Temperature (SIT). In order to remove the effect of external size of the AC particles on the properties measured, the samples to be tested were first crushed and finely sieved to have a uniform size. About 3-5 mg of crushed sample was tested under a continuous flow of oxygen/helium mixture (21/79). The sample was heated at 5 K/min from 30 °C to 650 °C and an isotherm at 105 °C for 30 minutes was used to remove adsorbed moisture from the carbonaceous sample. Further information on the methodology can be found from the work of Suzin *et al*.

Figure 3 shows an example of the shape of the net heat flux and mass evolution. The TG-DSC thermograms describe a continuous exothermic oxidation process ended by complete combustion of the sample. According to Suzin et al., the SIT was determined from the net heat flux curve measured, and corresponds to the temperature where the tangent to the point of inflection intersects the baseline DSC value. The PIO, represents the point at which the exothermic reaction is significant: a low oxidation process takes place with partial oxidation of the carbon and the organic components. The PIO was extracted from the net heat flux curve by locating the initial point of monotonic deviation from the baseline. Using this method the relative errors for the experimental determination of the SIT and PIO were estimated respectively to be less than 5 and 10 %.

Figure 3. TG-DSC thermograms of a physically activated carbon sample NC-60 showing heat and mass curves

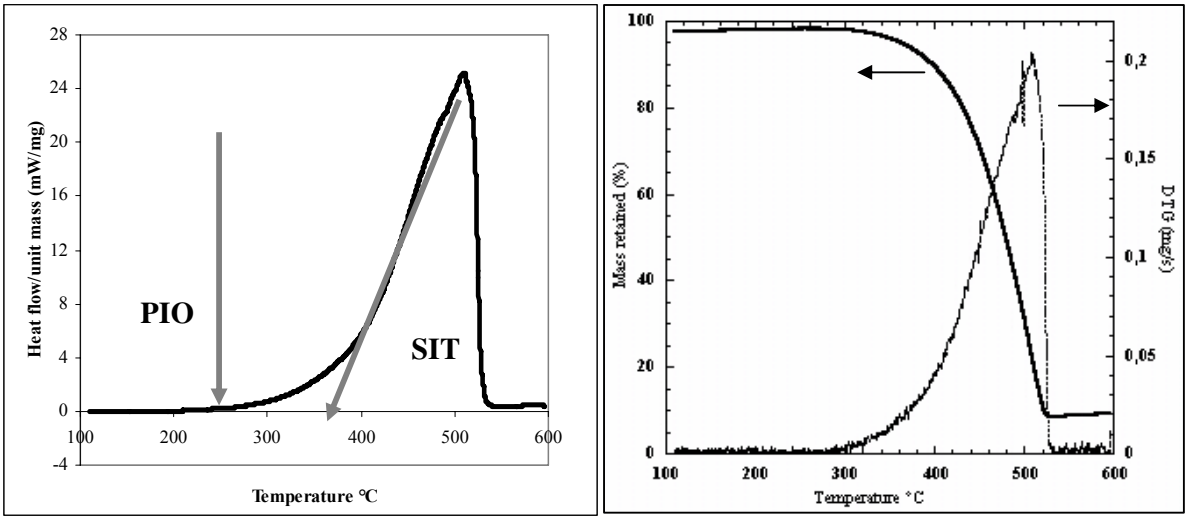

3. Results and discussions

3.1 Influence of oxygen to carbon ratio

The influence of oxygen to carbon ratio of activated carbons on the reactivity can be studied from the figure 4 where log (O/C) versus PIO and (O/C) versus SIT were plotted. Firstly there is an increase in the reactivity (lower PIO and SIT values) of the activated carbons samples with an increase in the oxygen to carbon ratio. The main reason is being attributed to the reactivity of the oxygenated surface functional groups with air. The oxygen content in activated carbons is present in the activated carbons in the form of surface oxygenated groups like carboxyl, hydroxyl, carbonyl, and ether groups (Boehm, 1994). Some of the oxygen content in the material may come from its origin and others from its activation mode. When activated carbons are exposed to air and heated,

the surface oxygenated groups reacts with air to form desorbable products like CO_2, CO, H_2O, intermediate complexes accompanied by exothermic heat (Hardman *et al*., 1983).

Looking at figure 4, there are exceptions to these trends found in activated coconut shell samples which have lower PIO values than expected. The deviation of the three activated coconut shell samples is shown in figure 4. An excellent regression coeffecient of 0.98 and 0.96 were obtained without the presence of these samples, with the presence of the coconut shell activated carbons the regression coefficients were much less significant with R^2 value of 0.58 and 0.47 for PIO and SIT respectively. Many reasons can be attributed for this behaviour, which may be due to higher affinity for the chemisorption of oxygen and especially the presence of higher potassium content in these samples which enhances the reactivity of the material (Bandosz and vander Merwe, 2005).

Figure 4. Effect of O/C ratio on the oxidation and ignition characteristics of activated carbons

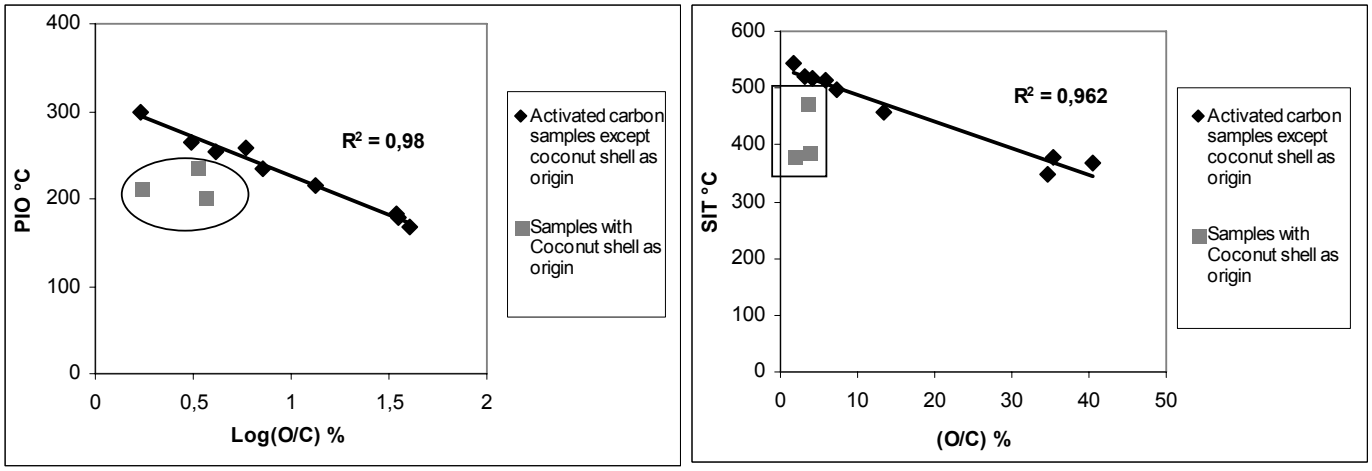

When the nitrogen rich activated carbons namely coal tar pitch and polyacrylonitrile fibre samples are compared with samples containing less nitrogen content, we find a global trend showing that the nitrogen rich samples are more stable and found to have higher PIO and SIT values. But since nitrogen and oxygen are both present particularly for the CTP and PAN based samples, it is difficult to show a tendency only for the nitrogen to carbon ratio versus PIO and SIT. The main reason for their stability seems to be the high temperature treatment involved in the activated carbon preparation which leads to thermally stable nitrogen substituting for carbon atoms in the ring system.

The effect of the O/C ratio on the reactivity is also demonstrated using the coal tar pitch and polyacrylo nitrile (PAN) fibre blend samples. The coal tar pitch (CTP) sample has an O/C ratio of about 1.7 % with a high PIO and SIT. On the other hand PAN-A has nearly 13.4 % O/C ratio approximately 8 times that of CTP sample with a lower PIO and SIT. The blends CTP-PAN gives cokes, which after activation have PIO and SIT depending upon the amounts of CTP and PAN in the blend. For example CTP-PAN-3:1-A resulting from the coking of 3 parts of CTP and one part of PAN has O/C of about 3.1 % compared to the activated carbon sample having 1 part of CTP and 1 part of PAN having relatively higher O/C of about 7.2 %. From the figure 5, it is evident that the reactivity of CTP-PAN-1:1-A is higher than that of CTP-PAN-3:1-A which shows that the presence of large proportion of CTP having lower oxygen content stabilizes the activated carbons from such blends.

Figure: 5 Influence of oxygen to carbon ratio on PIO and SIT values for coal tar pitch and polyacrylo nitrile fibre blend samples

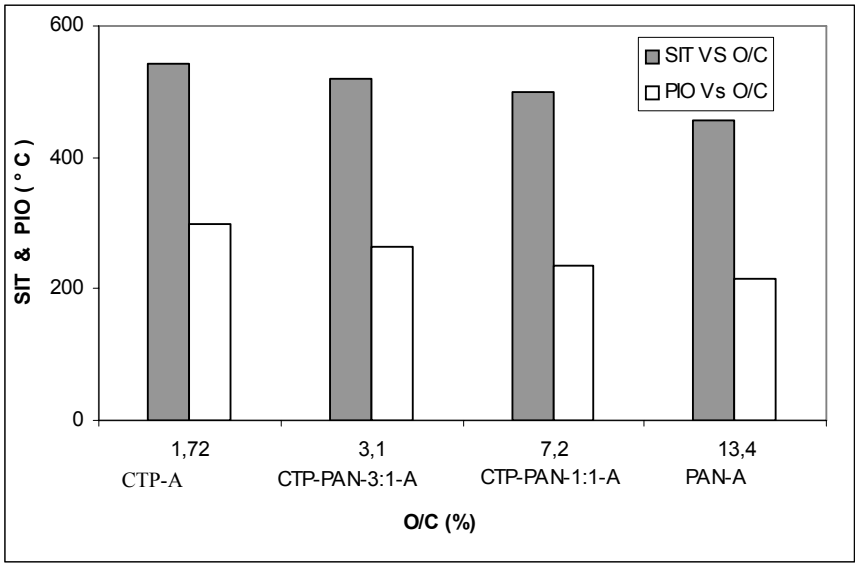

In order to verify the interpretation; that the increase of oxygen content in the carbon matrix increases the reactivity of the activated carbons, a complementary Temperature Programmed Desorption was carried out. The activated carbon samples were heated under an inert atmosphere like helium to about 750 °C to remove a part of the surface oxygenated groups. The oxygen content of the samples was then measured without exposing them to air. This was followed by Temperature Programmed Oxidation (TPO) in an atmosphere of oxygen. These experiments show there is a considerable increase in the PIO with a decrease in the oxygen to carbon ratio of the activated carbon samples previously subjected to TPD. This verifies the role of the surface oxygenated groups in the reactivity of the activated carbons.

Figure 6. Results of Temperature Programmed Desorption followed by oxidation of activated carbons

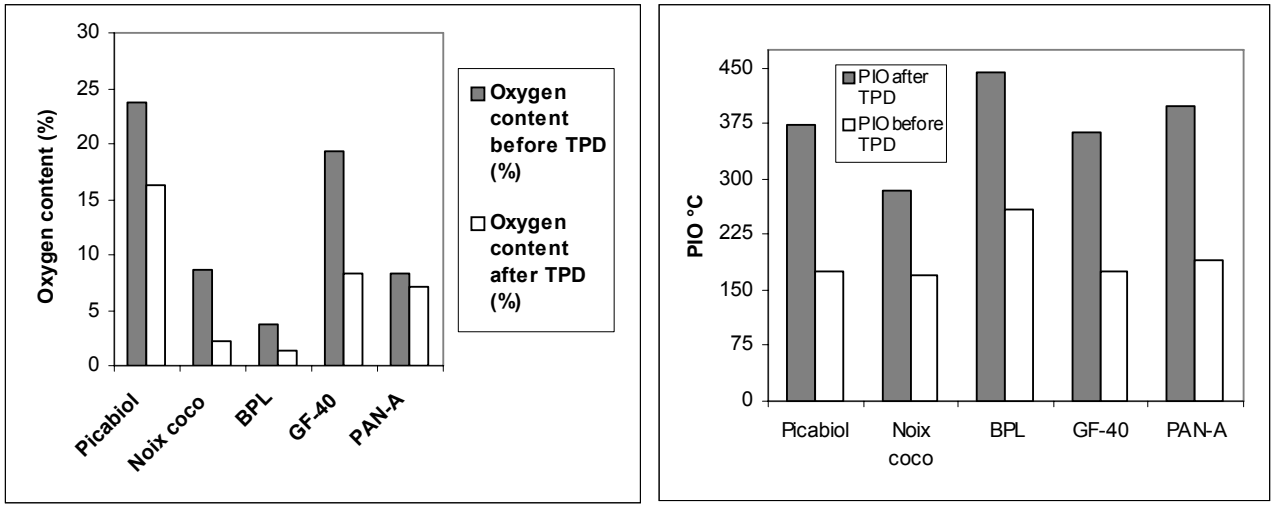

3.2. Influence of Porosity Characteristics

The porosity characteristics constitute important parameters like the specific surface area (S_{BET}), the porous volume (Vporous), the width of the micropore (Wmicro) and volume of micropores (Vmicro). However, no noticeable trends were observed with PIO and SIT.

3.3 Influence of structural properties

From the visual observation of the HRTEM images (Figure 2), we clearly find some differences in the structural organization among the carbon samples. Three distinct characteristics have been observed in the carbon samples analysed based on the fringe length, interlayer spacing and number of stacked layers in a coherent domain. The first group of carbon samples have short fringe length and the graphitic layers are randomly arranged in an isolated fashion without appreciable stacking of the layers (> 60 % NSL, i.e. non stacked layers). This feature is mainly seen in the chemically activated carbons, namely GF-40, Picabiol and BC-120. The main reason is being attributed to the mode of activation with a chemical agent and the low temperatures experienced during the process of manufacture. Aromatisation, i.e. formation of polyaromatic layers, and activation, i.e. grafting of oxygenated groups on the layers boundaries, occur concomitantly. Consequently, small and highly cross linked layers, are formed rending difficult the layer stacking. Therefore, in comparison with physically activated carbons, L and N are small, whereas d and % NSL are high. An important feature is that these samples have a high O/C ratio.

The second group of carbon samples show long graphitic sheets, weakly stacked (about 50 % NSL) and slightly bent constituting spaces between them as seen in activated carbon samples like NC-60, BPL, NC-100 and RB-2. These samples are physically activated at around 800 – 1000 °C and exhibit low oxygen to carbon ratio.

The third group of carbon sample contains mainly the coal tar pitch and polyacrylonitrile with a lamellar nanostructure of the graphitic layers which tend to be parallel to each other and better stacked compared to the first and second group of samples. The best example of this groups is the CTP based activated carbon (< 15 % NSL and L being the largest) This is due to CTP precursor which leads to a well ordered graphitisable coke with well stacked nanometer-sized layers giving a lamellar nanostructure (Rouzaud, 2004), and to the physical activation which do not induce noticeable cross-linking responsible for strong alteration of this nanostructure. The PAN precursor forming a non-graphitizable char give activated carbons which show a structure noticeably more disorganised than the CTP sample. The CTP-PAN samples which are a mixture of CTP and PAN precursors give physically activated carbons which take a character depending on the composition of the mixture.

The influence of the quantitative structural data on the reactivity of the activated carbon was then studied. The only well established tendency by graphical analysis is that of the graphitic layers (with fringe length greater than 4.9 A) to that of PIO. Looking at figure 7, we find the larger the graphitic layer length, the higher the PIO of the activated carbon samples. This is attributed to the presence of short distorted layers containing surface oxygenated groups at their boundaries which may be responsible for the early oxidation of the activated carbons. There are 2 exceptions namely BPL and RB-2 which do not fit into this tendency which may be due to the slight increase in the (O/C) ratio of these samples. The R^2 value of 0.95 is obtained without BPL and RB-2 samples.

Figure 7. Graphitic layer length of the carbon samples and their influence on PIO

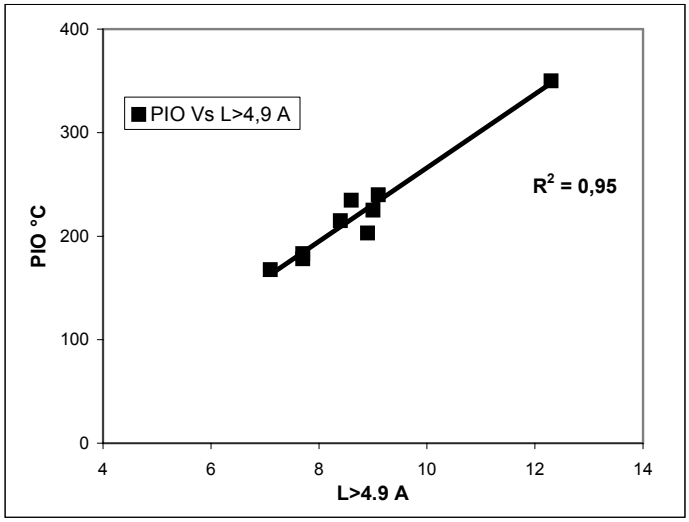

Other trends observed from the quantitative data like the % of non-stacked layers and N the number of stacked layers in a domain on the reactivity PIO and SIT. We find that the stable activated carbons have lower percentage of non-stacked layers and higher number of stacked layers in a domain which probably limit the accessibility of oxygen to active sites.

4. Statistical correlations

The quantitative statistical correlations were derived using multiple linear regression (MLR) technique. The type of MLR carried out is stepwise multiple linear regression using MINITAB software which consists in successive addition of the predictor variables at each stage to get a better coefficient satisfying all the statistical conditions. The MLR is done with the samples whose structural, textural and chemical properties are known. An important step that is the multicollinearity character which is the interdependence among the predictor variables is checked using matrix correlation (Giraudet *et al.*, 2006) and those pairs which are strongly correlated like V_{micro} and graphitic layer length with fringe greater than 2.85 Å and 4.9 Å are considered one at a time during regression analysis. This well agrees that the micropores are made up of weakly stacked layers.

Table 4. Matrix of correlation for predictor variables.

	O/C (%)	S_{BET} (m^2/g)	Vporous (cm^3/g)	Wmicro (nm)	Vmicro(cm^3/g)	L > 4.9 Å
S_{BET} (m^2/g)	0.57					
Vporous (cm^3/g)	0.66	0.69				
Wmicro (nm)	0.16	0.61	0.51			
Vmicro(cm^3/g)	0.27	0.07	0.44	0.36		
L > 4.9 Å	-0.62	-0.68	-0.65	0.11	**0.77**	
L > 2.85 Å	-0.53	-0.67	-0.61	0.11	**0.81**	**0.98**

$$\mathbf{PIO = 83.3 - 1.38\ O/C_{(\%)} + 27.5\ L_{>2.85\,(Å)}} \quad \textbf{with} \quad \mathbf{S = 15\ °C} \quad \mathbf{R^2 = 94\%}$$

The best regression for PIO was obtained with O/C ratio and graphitic layer length without the sample NC-60. The regression coefficient for (O/C) with PIO was only 0.60 which increases to 0.94 on addition of the graphitic layer length through the stepwise addition of predictor variables. The accuracy of the model is given by the R^2 value of 0.94 and the standard error of fits S of 15 °C. The magnitude of the individual properties cannot be directly interpreted from the regression equation due to the differences in the units of the predictor variables. As the predictor variables are in different units of measurement, the regression equation is computed again with the standardized data. The coefficients resulting from the standardized data (substracted from the mean and divided by standard deviation) are called as beta coefficients used directly for predicting the magnitude of the predictor variables on the response variables (Giraudet *et al*., 2006).

$$\mathbf{PIO = 0.69\ L_{>2.85\,(Å)} - 0.41\ O/C_{(\%)}}$$

From the beta coefficients, we find that the graphitic layer length is more influent than the oxygen to carbon ratio for the activated carbons considered. There was not a better coefficient for SIT with the predictor variables.

Figure: 8 Result of the prediction ability of the best multiple linear regression for PIO

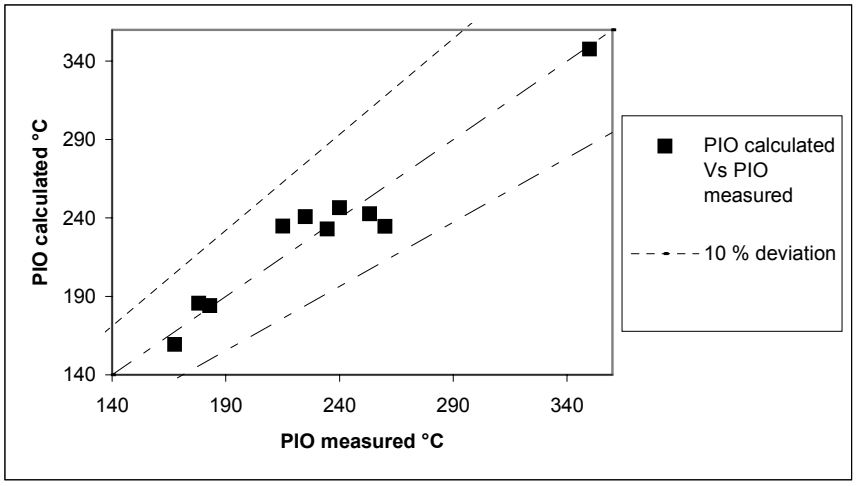

From the statistical correlation results, it was found that oxygen to carbon ratio and graphitic layer length influences PIO. The porosity characteristics like S_{BET} and Vporous influences in a less significant way and has not been put into evidence as the addition of the porosity characteristics deteriorated the coefficient of determination.

5. Conclusions

The oxidation and ignition characteristics of a large number of activated carbons having diversified origins and properties with different modes of activation were studied using TG-DSC techniques. The in house HRTEM analysis of the carbon samples provided information about the structural organisation of these carbons samples. Based on these qualitative and quantitative results, it was found that the graphitic layer length and oxygen to carbon ratio are the most important parameters influencing the oxidation and ignition of activated carbons. The porosity properties like the porous volume and the specific surface area also influence the reactivity but with a smaller magnitude, instead can be better explained with the structural properties. Though the properties of oxidation and ignition may change with experimental conditions, the results obtained here enable us to assess the properties influencing the reactivity of activated carbons under a given condition and there is still scope for improving the results by clubbing different structural properties.

References

Bansal, RC. Donnet, JB. Stoeckli, N. 1988. *Active Carbon. New York: Marcel Dekker* p. 10-49.

Boehm, HP. 1994. Some aspects of the surface chemistry of carbon blacks and other carbons. *Carbon* 2:759-769.

Bowes, PC. Cameron A. 1971. Self heating and ignition of chemically activated carbon. *J. Appl. Chem. Biotechnol* 21:244-250.

Lastoskie, C. Gubbins, KE. Quirke, N. 1993. Pore size distribution analysis of mcroporous carbon: A density functional theory approach. *J. Phys. Chem* 97:4786-4796.

Delage, F. Pré, P. Tezel, H. Le Cloirec, P. 2000. Mass transfer and warming during adsorption of high concentrations of VOC on an activated carbon bed: experimental and theortical analysis, *Environ. Sci Technol* 34:4816-4821.

EPA, 1997 Chemical Emergency Preparedness and Prevention office. Fire Hazard from carbon deodorizing systems. EPA 550-F-97-002 e.

Giraudet S, Pré P, Tezel H, Le Cloirec P. 2006. Estimation of the coupled influence of the porosity characteristics of activated carbons and the molecular properties of VOCs on the adsorption energy. *Carbon*, 44 :2413-2421.

Hardman, JS. Lawman, CJ. Street, PJ. 1983. Further studies of the spontaneous behaviour of activated carbon. *Fuel* 62:632-638.

Jones, JC. 1998. Towards an alternative criterion for the shipping safety of activated carbons. *Journal of Loss Prevention in Process Industries* 11:407-411.

Lillo-Rodenas, MA. Amoros, DC. Solano. AL, Béguin. F, Clinard, C. Rouzaud, JN. 2004. HRTEM study of activated carbons prepared by alkali hydroxide activation of anthracite. *Carbon* 42:1305-1310.

Lecloux, A. 1971. Exploitation of adsorption and desorption isotherms of nitrogen for the study of textural properties of porous solids. Mémoires société des sciences de Liège, Belgium, , tome I, fasc. 4, 169-209.

Machnikowski J, Grzyb B, Weber JV, Frackowiak E, Rouzaud JN, Béguin F. 2004. Structural and electrochemical characterisation of nitrogen enriched carbons produced by the co-pyrolysis of coal tar pitch with polyacrylonitrile. *Electrochimica Acta* 49:423-432.

Naujokas, AA. 1985. Spontaneous combustion of carbon beds. Plant/Operations Progress 4:120-126.

Olivier, JP. 1995. Modelling physical adsorption on porous and nanoporous solids using density functional theory. *J. Porous Mater* 2:9-17.

Rouzaud, JN. Christian, C. 2002. Quantitative high-resolution transmission electron microscopy: a promising tool for carbon materials characterization. *Carbon* 77-78:229-235.

Rouzaud, JN. 2004. The multiscale organization as a fingerprint of the formation conditions of carbons; a TEM study. Extended Abstracts Carbon, Providence, Rhode Island, USA.

Russell, NV. Gibbins, JR. Williamson, J. 1999. Structural ordering in high temperature coal chars and the effect on reactivity. *Fuel* 78:803-807.

Suzin, Y. Buettner, LC. LeDuc, CA. 1999. Characterizing the ignition process of activated carbon. *Carbon* 37:335-346.

van der Merwe, MM. Bandosz, J. 2005. A study of metal impregnated carbons: the influence of oxygen content in the activated carbon matrix. *J. Colloid Interface Sci* 282:102-108.

Zerbonia, RA. Brockman, CM. Peterson, PR. Housely, D. 2001. Carbon bed fires and the use of carbon canisters for air emissions control on fixed roof tanks. *J Air & Waste Management Assoc* 51:1617-1627.